



# New hyaluronan derivative with prolonged half-life for ophthalmological formulation

Gemma Leone<sup>a,\*</sup>, Marco Consumi<sup>b</sup>, Stefania Lamponi<sup>a</sup>, Agnese Magnani<sup>a</sup>

<sup>a</sup> Department of Pharmaceutical and Applied Chemistry, University of Siena, Via Aldo Moro 2, 53100 Siena, Italy

<sup>b</sup> ALTA S.r.l.u., Via Fiorentina 151, 53100 Siena, Italy

## ARTICLE INFO

### Article history:

Received 7 October 2011

Received in revised form

19 December 2011

Accepted 24 December 2011

Available online 24 January 2012

### Keywords:

Hyaluronan

Phosphorylation

Viscosity

Enzymatic degradation

## ABSTRACT

Two new hyaluronan derivatives containing phosphate or cystamine groups have been synthesised to obtain tear drops with improved rheological properties and prolonged half-life. Rheological analysis, in terms of apparent viscosity, pointed out that phosphorylated hyaluronan showed promising characteristics for the foreseen application. The presence of phosphate groups along the chains, confirmed by infrared analysis, induced a strengthening in hyaluronan hydrogen bond capability thus modifying its thermal behaviour and prolonging its resistance against hyaluronidase attack. Finally, in vitro cytotoxicity tests excluded any adverse effect of the developed hyaluronan derivative.

© 2012 Elsevier Ltd. All rights reserved.

## 1. Introduction

Eye drops are commonly instilled to treat a variety of ocular problems, such as dry eyes, glaucoma, infections, allergies, despite their short contact time with the eye surface, which results in reduced effects for artificial tears or low bioavailability for ophthalmic drugs (Maurice, 1973). In fact, if the instilled fluid has a viscosity similar to that of tears, which is about 1.5 mPa s, the instilled fluids or solutes are eliminated from the tears in few minutes (Snibson et al., 1990; Yokoi & Komuro, 2004). To increase the duration of comfort after drop instillation or to increase the bioavailability of the drugs, it is desirable to prolong the residence time for the instilled fluid. It has been shown in a number of clinical and animal studies that the retention began to increase only after the fluid viscosity exceeded a critical value of about 10 mPa s (Zaki, Fitzgerald, Hardy, & Wilson, 1986; Zhu & Chauhan, 2008). Although increasing fluid viscosity increases the residence time, it may also cause discomfort and damage to ocular epithelia due to an increase in the shear stresses during blinking.

Natural macromolecules such as hyaluronan (HA), present in the vitreous body of the eye, have been proposed as viscosifying agents. Sodium hyaluronate has physical properties and a composition comparable to tear glycoproteins and easily coat the corneal epithelium. The non-Newtonian behaviour of sodium hyaluronate

combines the advantage of high viscosity at rest between blinks with those of lower viscosity during blinking (Ludwig, 2005).

Diluted solutions of sodium hyaluronate have been employed successfully as tear substitutes in severe dry eye disorders. The beneficial effects are attributed to the viscoelasticity, biophysical properties similar to mucins, providing a long-lasting hydration and retention. Moreover, good lubrication of the ocular surface is obtained (Ludwig, 2005).

However, one of the disadvantage of actually commercialised preparations based on HA is the very short half-life due to the hyaluronidase attack, being degraded within the first 3 h.

The aim of this study is the development of new hyaluronan derivatives with improved rheological properties as tear drops and with a longer half-time with respect to native hyaluronan.

Two different derivatives were synthesised by the introduction of phosphate and cystamine groups along the chain. Both phosphate and amino groups should increase the hydrophilicity of polysaccharide (Barbucci et al., 2005). The effect of these new functionalities on the rheological properties and the enzymatic degradation rate was evaluated as well as their cytotoxicity.

## 2. Materials and methods

### 2.1. Materials

Sodium salt of hyaluronan (MW  $1.2 \times 10^6$ ) was received as a gift from SIFI S.p.A (Italy).

\* Corresponding author.

E-mail address: [leone10@unisi.it](mailto:leone10@unisi.it) (G. Leone).

All the materials and reagents were purchased from Fluka Sigma Aldrich (Switzerland) and used without further purification. All the solvents were of analytical or HPLC grades.

## 2.2. Methods

### 2.2.1. Synthesis of phosphorylated hyaluronan (HAP)

The polysaccharide was solubilised in bidistilled water to a final concentration of 1% (w/v). The pH was raised to 11.5 by adding sodium hydroxide (0.1 M). After 5 min the solution was transferred in a saturated sodium trimetaphosphate (STMP) solution (20% (w/v) pH 12.5) drop by drop maintaining vigorous stirring at room temperature and the pH was adjusted to about 7.0 with HCl 0.1 M. After 2 h the phosphorylated derivative of HA was precipitated in ethanol and then dissolved in bidistilled water. The solution was dialysed against water for 48 h, and lyophilised.

The phosphorylation degree was determined by a spectrophotometric assay using a commercial kit (Test Spectroquant Merck KqaA – Darmstadt – Germany – ISO6878/1 and US-standard Methods 4500-P-E) following the producer instruction. To perform the analysis the sample was heated up to 700 °C and the obtained residue was quantitatively collected for the phosphate assay. The residue was treated with a drop of concentrated sulphuric acid. After 15 min 2 mL of bidistilled water were added and the sample was sonicated for 30 min. Then, the resulting solution was quantitatively transferred in a volumetric flask. This procedure was repeated three times.

A calibration curve was obtained from a standard phosphate solution. Using diluted standard phosphate solutions ranging from 0.1 to 6 mg/L (stock solution 1000 mg/L, 1:10 dilution steps), the linear region of the assay was found to range from 0.1 to 4 mg/L.

The phosphorylation degree was expressed as the % of P per mg of polysaccharide (Magnani, Rossi, Consumi, & Greco, 2010).

### 2.2.2. Synthesis of cystaminic hyaluronan (PAHAC)

**2.2.2.1. Polyaldehydic hyaluronan (PAHA).** HA was oxidised by sodium periodate to introduce aldehyde groups. Briefly, 500 mg of HA were dissolved in 10 mL of bidistilled water. Sodium periodate (60 mg) was added to the solution. The mixture was stirred at room temperature in the dark for 4 h. Ethylene glycol (1 mL) was then added to inactivate unreacted periodate. The resulting solution was dialysed against bidistilled water, lyophilised and stored at –20 °C. The substitution degree was determined by NMR spectroscopy (Jia et al., 2004). Briefly, the periodate-oxidised HA (PAHA) was dissolved in an acetate buffer (pH 5.2) at a concentration of 10 mg/mL. A 5-fold excess of tert-butyl carbazate (TBC) and sodium cyanoborohydride ( $\text{NaBH}_3\text{CN}$ ) was dissolved in the same buffer and added separately. The mixture was allowed to react for 24 h at room temperature. The polymer was recovered by precipitation in acetone three times. The polymer was further purified by dialysis against 0.1 M NaCl solution and bidistilled  $\text{H}_2\text{O}$ . The freeze-dried product was subjected to  $^1\text{H}$  NMR examination, and the aldehyde content was calculated comparing the signals at 1.4 ppm (9H, carbazate t-Boc) and 1.9 ppm (3H, HAox acetamide).

**2.2.2.2. Cystaminic hyaluronan (PAHAC).** PAHA was further modified by the introduction of cystamine residues. 100 mg of PAHA were dissolved in 2 mL of PBS (pH 8). Cystamine was added to the mixture in a molar ratio 1:2 with respect to aldehyde moieties and the reaction was left under stirring for 12 h. The solution was purified by ultracentrifugation (cut-off 30000 Da).

The presence of unreacted aminic groups, which points out the presence of cystamine residues along the hyaluronan chains, was verified by ninhydrin assay (Virender, Kent, Tam, & Merrifield, 1981).

### 2.2.3. Physico-chemical characterisation

**2.2.3.1. Infrared analysis.** FTIR spectra of dried polymers were recorded on a Nicolet Thermo 5700 apparatus equipped with an attenuated total reflection (ATR) accessory and a 45° Germanium crystal as internal reflection element. The spectra were acquired between 4000 and 750  $\text{cm}^{-1}$ . A MCT (Mercury–Cadmium–Tellurium) detector was used, and the apparatus was purged with nitrogen. Typically, 64 scans at a resolution of 2.0  $\text{cm}^{-1}$  were averaged. The frequency scale was internally calibrated with a helium–neon reference laser to an accuracy of 0.01  $\text{cm}^{-1}$ . FTIR spectra were corrected using the OMNIC™ correction ATR software to take account of spectral changes due to the variation of the IR beam penetration depth into as a function of wavelength. For additional verification of the band assignments, spectra were processed with the second-order Savitzky–Golay method with 11 convolution points used to generate the second derivative of the spectra.

**2.2.3.2. Rheological characterisation.** The apparent viscosity of the samples (2 mL) was determined by shear rate experiments in a range  $D = 1\text{--}100\text{ s}^{-1}$  using a controlled strain rheometer equipped with a concentric cylinders system (AR2000, TA Instruments, Leatherhead, United Kingdom). All the measurements were performed at 37 °C.

Intrinsic viscosity was determined following the procedure reported by Cowman and Matsuoka (2005).

**2.2.3.3. Thermogravimetric analysis.** Thermogravimetric analysis (TGA) was performed on Q600 thermogravimetric analyzer (TA Instruments–Waters, USA). Samples (5–10 mg) were put in a steel crucible and heated from room temperature to 700 °C, with a rate of 10 °C/min, under air purge gas.

**2.2.3.4. In vitro cytotoxicity, cell proliferation and viability.** To evaluate the in vitro cytotoxicity and ability to influence cell proliferation of polymers, the direct contact test, proposed by “ISO 10993-5 biological evaluation of medical devices – Part 5: tests for cytotoxicity: in vitro methods”, was utilised. This test is suitable for samples with various shapes, sizes or physical states (i.e. liquid or solid).

Mouse tumoral fibroblasts NIH3T3 were utilised for cytotoxicity, cell proliferation and viability experiments. NIH3T3 fibroblasts were propagated in Dulbecco's modified Eagle's medium (DMEM) supplemented with 10% foetal calf serum, 1% L-glutamine–penicillin–streptomycin solution, and 1% MEM non-essential amino acid solution, at 37 °C in a humidified atmosphere containing 5%  $\text{CO}_2$ . Once at confluence, cells were washed with PBS 1 ×, taken up with trypsin–EDTA solution and then centrifuged at 1000 rpm for 10 min. The pellet was re-suspended in complete DMEM solution (dilution 1:15).

## 2.3. Seeding of cells

The cytotoxicity test was performed by two different techniques in order to analyse the influence of polymers on cell adhesion too.

100  $\mu\text{L}$  of 1% (w/v) polymer solution in PBS, previously filtered by 0.22  $\mu\text{m}$   $\varnothing$  filters, were added to 900  $\mu\text{L}$  of cell suspension in complete medium containing  $1.5 \times 10^3$  cells. Then cell suspension was seeded in each well of a 24 well round multidish and incubated at 37 °C in an atmosphere of 5%  $\text{CO}_2$ . (method 1)

$1.5 \times 10^3$  cells suspended in 1 mL of complete medium were seeded in each well of a 24 well round multidish and incubated at 37 °C in an atmosphere of 5%  $\text{CO}_2$ . Once cells reached the 50% of confluence (i.e. after 24 h of culture) the culture medium was discharged and 900  $\mu\text{L}$  of fresh complete medium added with 100  $\mu\text{L}$  of 1% (w/v) polymer solution in PBS, previously filtered by 0.22  $\mu\text{m}$   $\varnothing$  filters, were added to each well. (method 2).

HDPE was used as negative control; organo-tin-stabilized poly(vinyl(chloride) (PVC) was used as positive control. All samples were set up in triplicate.

#### 2.4. Evaluation of cell proliferation and viability

The number of cells in contact with polymer was evaluated by an inverted optical microscopy (IX 50, Olympus, Germany) at the following intervals: 24, 48 and 72 h. Cells were counted directly or by previous fixing in 2.5% glutaraldehyde in 100 mM sodium cacodylate and staining by trypan blue. Images of cells in contact with hydrogels were captured by a digital camera applied to the microscope (Camedia C5050, Olympus, Germany).

#### 2.5. Statistical analysis

Multiple comparison were performed by one-way ANOVA and individual differences tested by Fisher's test after the demonstration of significant intergroup differences by ANOVA. Differences with  $p < 0.05$  were considered significant.

##### 2.5.1.1. Enzymatic degradation

Buffered solutions of modified hyaluronan and native hyaluronan (as control) were prepared by dissolving 15  $\mu$ g of polysaccharide in 1.0 mL of ammonium acetate at physiological pH. The solutions were kept at 37 °C in a thermostatic bath and hyaluronidase (Sigma) was then added to digest hyaluronic acid providing uronic acid. The test was performed on the basis of the method of Saad, Myers, Castleton, and Leary (2005).

Each sample was added of an excess of hyaluronidase and the amount of uronic acid obtained during the digestion period was determined spectrophotometrically via the carbazol test (Bitter & Muir, 1962; Hedberg, Shih, Solchaga, Caplan, & Mikos, 2004). Briefly, 100  $\mu$ L of the degradation solution were added to a solution containing concentrated sulphuric acid and sodium tetraborate decahydrate. The solution was heated up to 100 °C over 10 min. Then, a solution of carbazol in pure ethanol (0.125% (w/v)) was added and the mixture heated up to 100 °C over 15 min. The absorbance of the solution ( $\lambda = 530$  nm) was determined by an UV–visible spectrophotometer (Perkin-Elmer lambda 25). Each experiment was done in triplicate.

### 3. Results and discussion

#### 3.1. Synthesis of phosphorylated hyaluronan (HAP)

The synthesis procedure is reported in Scheme 1A (supplementary data).

High molecular weight HA was chosen since it is an essential requirement for the prolonged residence time of the substance on eye (Durrani, Farr, & Kellaway, 1995).

STMP can be used both as a phosphorylating or a crosslinking agent. The mechanism is assumed to be organised in the opening of the STMP cycle by one hydroxyl group of hyaluronan chains in the presence of sodium hydroxide. At high concentrations of the polymer (more than 1%) the addition of a new polymer chain was favoured, thus affording the crosslinking with the release of pyrophosphate whereas in dilute solution (i.e. 1%) the attack by a hydroxyl group of the same unit is more probable (Leone, Torricelli, Giardino, & Barbucci, 2008; Leone et al., 2010). Furthermore, the solvent choice is fundamental, sodium chloride screens the carboxylate charges and as a result brings macromolecular chains closer, thus favouring the crosslinking process; at basic pH, instead, the charged carboxylate groups provoke a repulsion among the chains, so that attack by a hydroxyl group of the same disaccharidic unit is favoured when a diluted solution in bidistilled water

is realised (Dulong et al., 2004; Ravanelle, Marchessault, Legare, & Buschmann, 2002).

The reaction time was reduced to minimise the hydrolysis. Kragten, Leeftang, Kamerling, and Vliegenthart (1992) demonstrated that in extremely basic conditions the polysaccharide hydrolysis take place after hours. The exposure of our polysaccharide to basic condition was 5 min so the integrity of the polysaccharide was preserved.

The phosphorylation degree, obtained as reported in Section 2.2.1, was  $6.7 \pm 0.3\%$  of P per mg of polymer.

#### 3.2. Synthesis of cystaminic hyaluronan (PAHAC)

A particularly common method in biology and biochemistry is the PAS-(periodate-Schiff base)-staining method for carbohydrates, the basis of which is the reaction between the Schiff reagent and aldehydes formed by periodate oxidation Scheme 1B (supplementary data). For oxidation of vicinal diols to occur, it is required that the OH groups were oriented in an equatorial–equatorial or axial–equatorial position. Vicinal OH groups in a rigid axial–axial position cannot react because the intermediate complex formation cannot take place.

Hyaluronan contains vicinal hydroxyl groups that can readily be modified with periodate to form aldehyde groups. The oxidised hyaluronan bearing aldehyde groups can react with any substance with free amino groups. The aldehyde groups on PAHA formed Schiff base with the free amino groups on the cystamine residues, leading to the formation of hyaluronan enriched with pendent amine groups.

The fundamental aspects of periodate oxidation have been thoroughly reviewed and a limited oxidation (typically less than 20%) of polysaccharides was found (Kristiansen, Potthast, & Christensen, 2010). The NMR data obtained on the sample confirmed this result. The oxidation degree of PAHA was  $16.7 \pm 0.8\%$  as determined by  $^1\text{H}$  NMR.

#### 3.3. Infrared analysis

Infrared analysis of native and modified linear polysaccharides was performed to verify the introduction of the new functional groups along the chains. The high signal-to-noise ratio of a FTIR spectrum gives the possibility to enhance the resolution of bands broader than the instrumental resolution. One of the most applied resolution enhancement methods is taking the second derivative of a FTIR spectrum, an approach widely used in peak identification and library search software (DeNoyer & Dodd, 2002; Griffiths & De Haset, 2007; Smith, 1996). In fact, it is known that the second derivative can identify the number of overlapped bands and the exact frequencies of peak response, based on its ability to clarify changes in the slope within the original spectrum (Smith, 1996; Griffiths & De Haset, 2007). Applying the second-order Savitzky–Golay method to generate the second derivative of the FTIR spectra results in the resolution of each broad band into sharper downward pointing bands.

The infrared spectra of phosphorylated (HAP) and native polysaccharide (HA) are reported in Fig. 1. The main wavenumbers observed in the IR spectra are summarised in Table 1 together with their assignments. Basing on Haxaire, Marechal, Milas, and Rinaudo (2003) all the bands of native HA (Fig. 1 grey curve) can be clearly identified and assigned. The broad band centred at  $3340\text{ cm}^{-1}$  corresponds to the OH stretching deriving from alcohols and hydrogen bonded N–H groups whereas the bands at  $2920$  and  $2850\text{ cm}^{-1}$  can be assigned to asymmetric and symmetric stretching of  $\text{CH}_2$  moieties, respectively. A very small band was centred at  $1740\text{ cm}^{-1}$ . This band can be related to the C=O stretching of free carboxylic group COOH in hyaluronic acid, since at pH 7.4 hyaluronan shows

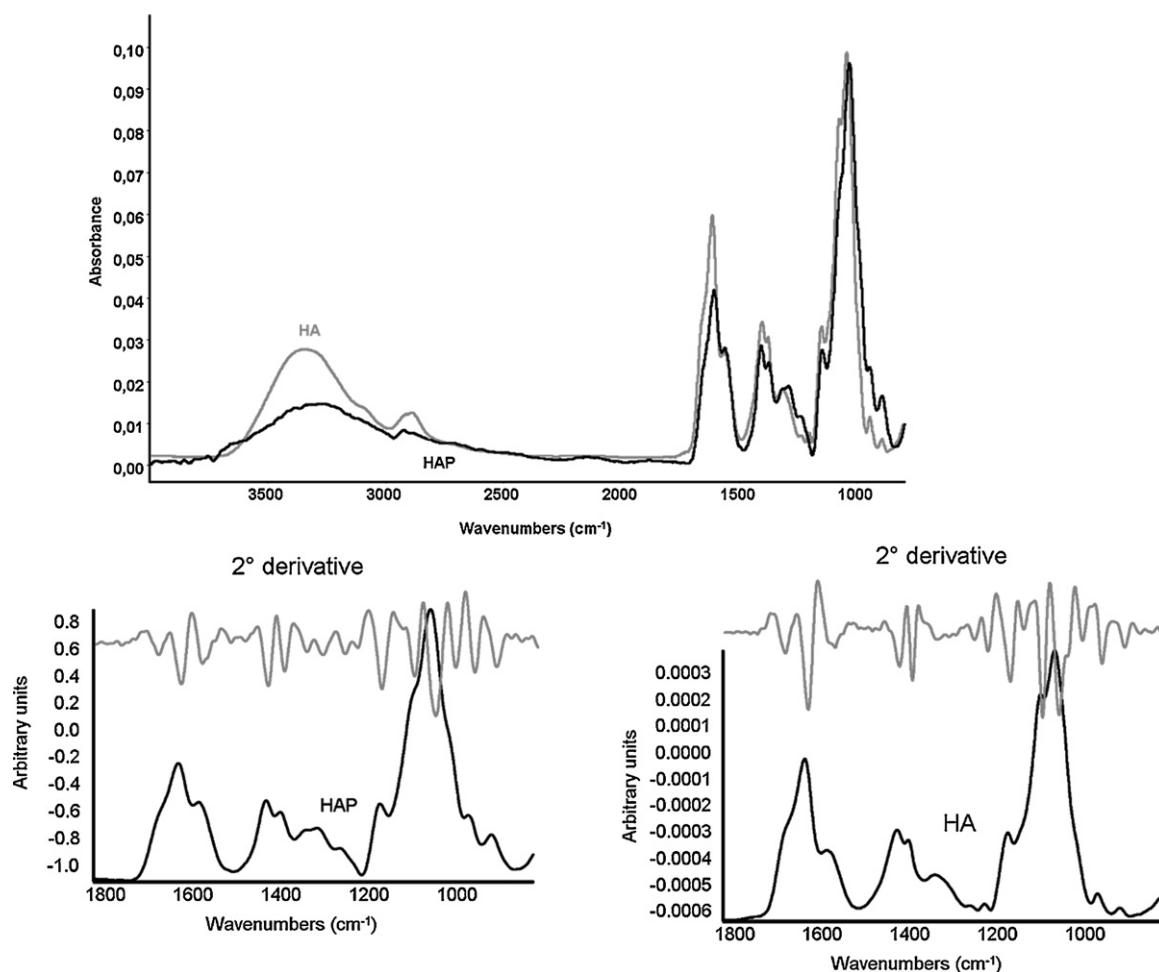


**Fig. 1.** (A) Infrared spectra of HA (grey curve) and HAP (black curve); (B) second derivative of HAP spectrum in the region 1800–900; (C), (B) second derivative of HA spectrum in the region 1800–900.

a small percentage of protonated carboxylic moieties (Barbucci, Consumi, & Magnani, 2002). This small band is accompanied by an intense broad band centred at  $1610\text{ cm}^{-1}$  which is relative to the asymmetric stretching of  $\text{C}=\text{O}$  of carboxyl  $\text{COO}^-$  group accepting one or two hydrogen bonds. The carboxylate band showed two shoulders centred at  $1662\text{ cm}^{-1}$  and  $1550\text{ cm}^{-1}$  which are relative to amide I (mainly stretching of amide  $\text{C}=\text{O}$  group accepting one or two hydrogen bonds) and amide II (mainly bending of amide  $\text{NH}$  group establishing one hydrogen bond), respectively. The broadness and low intensity of the amide groups bands could be assigned to the multiple bands convolved inside due to the involving of these chemical groups in a strong and complex hydrogen-bond network.

The presence of carboxylate moieties was confirmed by the band centred at  $1404\text{ cm}^{-1}$  deriving from the symmetric stretching of carboxylate  $\text{C}=\text{O}$  moieties. Finally, a significant broad band in the region  $1150\text{--}1040\text{ cm}^{-1}$ , relative to saccharidic unit is present. The specific assignments of all the contributions to this band, highlighted by the second derivative, are reported in Table 1.

The infrared spectrum of phosphorylated HA (Fig. 1 black curve) was similar to that of native HA. The main difference between the infrared spectrum of native and phosphorylated HA was the presence of a double band centred at  $1293\text{ cm}^{-1}$  and  $1276\text{ cm}^{-1}$ , which deserves close discussion. The nearest HA native band located at  $1315\text{ cm}^{-1}$  is not close enough in frequency and is too weak in intensity to account for the feature at  $1293\text{ cm}^{-1}$ . On the other hand, it has been well documented that IR spectra of organophosphates often contain a characteristic band at  $1295\text{ cm}^{-1}$ , which arises

from the non-hydrogen-bonded  $\text{P}=\text{O}$  groups (Bellamy, 1980; Frey, Hanken, & Corn, 1993; Thomas & Chittenden, 1964). Therefore, we assigned the absorbance at  $1293\text{ cm}^{-1}$  to the  $\text{P}=\text{O}$  stretching mode in the absence of hydrogen bonding. Furthermore, the bands centred at  $990$  and  $1080\text{ cm}^{-1}$ , due to  $\text{PO}(\text{H})$  and  $\text{PO}(\text{C})$  stretching vibrations, respectively, contributed to the increase of the absorbance due to the  $\text{COH}$  and  $\text{C}-\text{O}-\text{C}$  ring vibrations mode.

Phosphate groups induced a strengthening in the hydrogen-bond capability of the amide groups as evidenced by the shift of the IR bands from  $1662\text{ cm}^{-1}$  to  $1656\text{ cm}^{-1}$  and from  $1550\text{ cm}^{-1}$  to  $1557\text{ cm}^{-1}$ , respectively. On the contrary, the carboxylic groups were more free from hydrogen-bonds as evidenced by the shift of the carboxylate group absorption band from  $1610\text{ cm}^{-1}$  to  $1623\text{ cm}^{-1}$ , and from  $1404\text{ cm}^{-1}$  to  $1415\text{ cm}^{-1}$ . Finally, the drastic decrease of the large shoulder centred at  $3400\text{ cm}^{-1}$  can be attributed to the involvement of OH groups in phosphorylation.

In Fig. 2 the infrared spectrum of native (HA), polyaldehydic HA (PAHA) and PAHA modified by the introduction of cystamine residues (PAHAC) are reported. The main wavenumbers observed in the IR spectra are summarised in Table 1 together with their assignments.

The PAHA spectrum showed a significant band centred at  $1725\text{ cm}^{-1}$  which can be related to aldehydic carbonyl group stretching which was absent in the IR spectrum of native HA. Thus, it confirms the successful occurrence of the first step reaction. The IR spectrum of PAHAC was characterised by the appearance of a new small shoulder centred at  $1470\text{ cm}^{-1}$  due to the  $\text{C}=\text{N}$  stretching



**Table 1**

Main wavenumbers observed in the FTIR spectra of native and derivatised HAs together with their assignments.

Samples	Wavenumbers (cm <sup>-1</sup> )	Assignments
HA	3340	Intra and inter molecular bonded OH stretching+ hydrogen bonded N—H stretching
	2920	CH <sub>2</sub> asymmetric stretching
	2850	CH <sub>2</sub> symmetric stretching
	1740	Free COOH stretching
	1662	Amidic CO stretching
	1610	COO <sup>-</sup> asymmetric stretching
	1550	NH bending
	1404	COO <sup>-</sup> symmetric stretching
	1147, 1080, 1042	Emiacetalic system (C—O—C) saccharidic unit
HAP	3340	Intra and inter molecular bonded OH stretching+ hydrogen bonded N—H stretching
	2920	CH <sub>2</sub> asymmetric stretching
	2850	CH <sub>2</sub> symmetric stretching
	1656	Amidic CO stretching
	1623	COO <sup>-</sup> stretching
	1557	NH bending
	1415	COO <sup>-</sup> symmetric stretching
	1293, 1276	PO <sub>3</sub> stretching
	1147, 1080, 1042	Emiacetalic system (C—O—C) saccharidic unit
PAHA	3340	Intra and inter molecular bonded OH stretching+ hydrogen bonded N—H stretching
	2920	CH <sub>2</sub> asymmetric stretching
	2850	CH <sub>2</sub> symmetric stretching
	1725	Aldehydic C=O stretching
	1648	Amidic CO stretching
	1546	NH bending
	1147, 1080, 1042	Emiacetalic system (C—O—C) saccharidic unit
PAHAC	3340	Intra and inter molecular bonded OH stretching+ hydrogen bonded N—H stretching
	2920	CH <sub>2</sub> asymmetric stretching
	2850	CH <sub>2</sub> symmetric stretching
	1648	Amidic CO stretching
	1546	NH bending
	1470	C=N Stretching (imine)
	1147, 1080, 1042	Emiacetalic system (C—O—C) saccharidic unit

deriving from the imine group which was formed by the reaction of cystamine residue with aldehydic function. A confirmation of the second step of hyaluronan modification was obtained. The absence of significant crosslinking among the PAHA chains after the cystamine introduction was demonstrated by the solubility of PAHAC polymer in water. Furthermore, ninhydrin assay indicated the presence of aminic groups, thus confirming the prevalent one side attachment of cystamine to the polymer chains.

### 3.4. Rheological analysis

The polymer viscosity is a parameter of great interest for assessing tear film stability and physiological compatibility. A higher viscosity compared with natural tears (1.5 mPa s) is, in fact, one of prerequisites for artificial tears. Nevertheless, the viscosity should not exceed 30 mPa s to not induce unpleasant feeling for the patient. Another requisite for artificial tears is the use of a newtonian or weak pseudoplastic system (Oechsner & Keipert, 1999). According to Chrai and Robinson a pseudoplastic behaviour can be a disadvantage compared to a newtonian solution which retains its viscosity during blinking (Chrai & Robinson, 1974). However, hyaluronan even though it is a pseudoplastic or shear thinning substance for its intrinsic bioadhesive and lubricating properties appears as an optimal polymer (Ludwig & Van Ooteghem, 1989).

Shear thinning fluids such as sodium hyaluronate (NaHA) solutions can be used to obtain the beneficial effect of an increase in retention and yet avoid excessive stresses during blinking (Snibson et al., 1990). The reason is that the shear rates during blinking are very high and at such high shear rates these shear-thinning fluids exhibit low viscosity, but during the interblink which is the period when tear drainage occurs, these fluids act as high viscous fluids leading to reduced drainage rates and a concurrent increase in residence time (Zhu & Chauhan, 2008).

To verify that the developed preparation fulfil all these requirements, a flow step analysis was performed.

The shear rate ( $D$ ) on the cornea may differ considerably. In fact, it changes in the range 1–10,000 s<sup>-1</sup>. When the eyes are open, the shear rate depends on the gravitation only and it can be valued approximately 1 s<sup>-1</sup>. During blinking the shear rate is around 10,000 s<sup>-1</sup>. The apparent viscosities of HA, HAP, PAHAC and commercial artificial tears, determined by controlled shear rate experiments in a range 1–100 s<sup>-1</sup>, were reported in Fig. 3A–D. Applying the Ostwald model, or Power law model, to the four formulation viscosity curves, the rate index  $N$ , also called fluidity index, can be obtained and subsequently the apparent viscosity for “blinking shear rate” can be calculated using the following formula (Oechsner & Keipert, 1999):

$$\eta_A = K \cdot D^{(N-1)}$$

where  $K = \eta_A$  for  $D = 1 \text{ s}^{-1}$

The fluidity index and the apparent viscosity at a shear rate of 1, 100 and 10,000 s<sup>-1</sup> are summarised in Table 2.

It can be seen that the calculated viscosities of the modified HA solutions are significantly higher than that of natural tears and native HA, reaching the threshold value of 10 mPa s which has been demonstrated to be the critical value from which retention began. However, to overcome a sticky sensation, blurred vision and reflex blinking due to discomfort or even irritation the viscosity should not be more than 30 mPa s at a shear rate of 10,000 s<sup>-1</sup>.

The fluidity index of all the analysed formulation are high and close to 1 pointing out a weak pseudoplastic behaviour with the exception of PAHAC which, having a fluidity index higher than 1 (1.4031) appears as a shear thickening or dilatant system. This difference can be attributed to the fact that a very low amount of crosslinking points are present. Consequently, at high shear rate

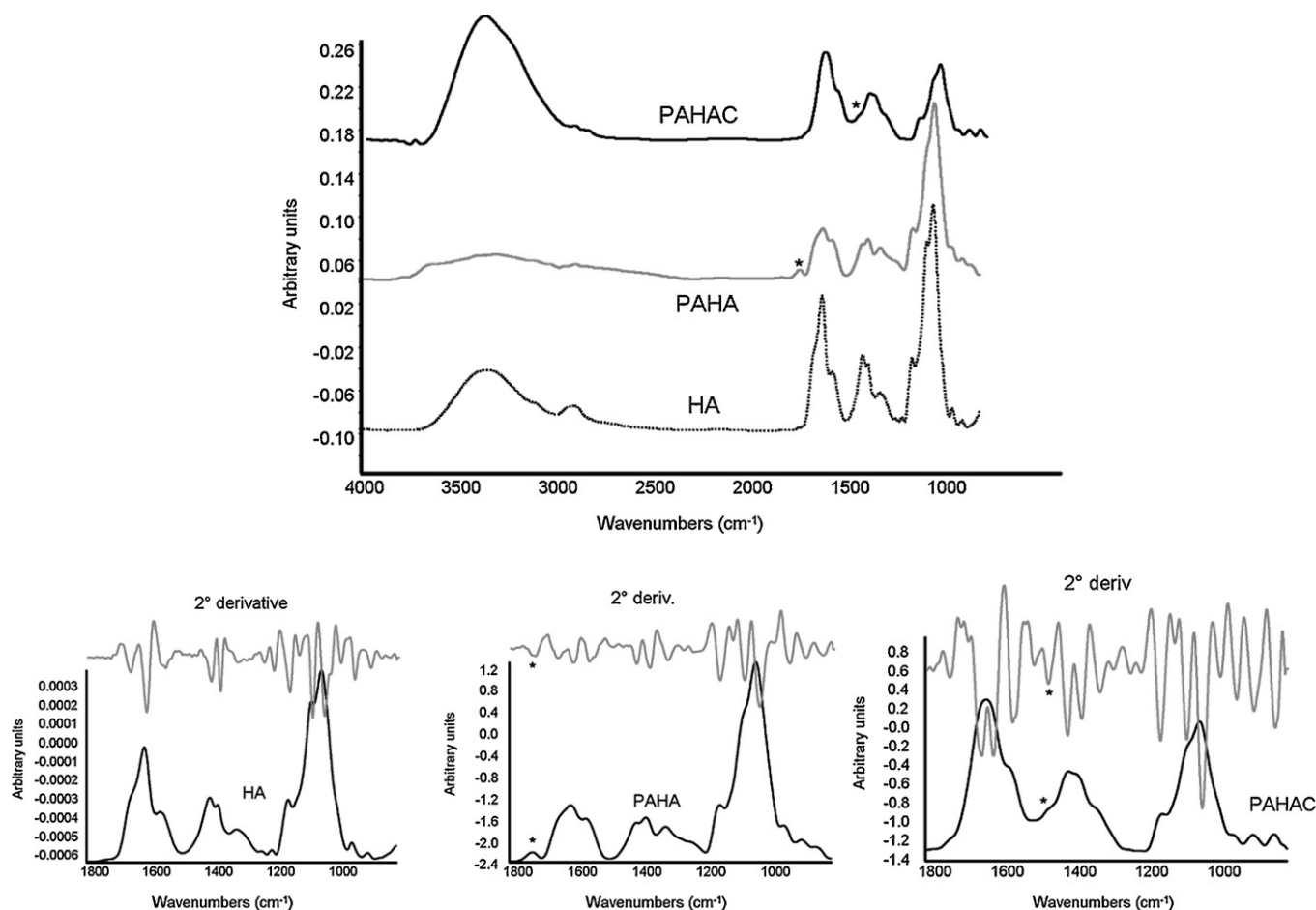


**Fig. 2.** (A) Infrared spectra of HA (black dot curve) PAHA (grey curve) and PAHAC (black curve); (B) second derivative of HA spectrum in the region 1800–900; (C), (D) second derivative of PAHA spectrum in the region 1800–900; D: second derivative of PAHAC spectrum in the region 1800–900.

( $D = 10,000 \text{ s}^{-1}$ ) the fluid comes out from the matrix and a hardening of the structure is observed.

Since the molecular weight has a deep effect on polymer rheological behaviour the effect of functionalisation procedure on native hyaluronan molecular weight was analysed. Firstly, to confirm that no polymer degradation occurred during the phosphorylation procedure, 0.1 g of hyaluronan was dissolved in basified water (pH 11.5 NaOH 0.1 M) and its viscosity monitored versus time. A period of 45 min occurred to observe a first small drop in viscosity.

Nevertheless, to determine the molecular weight of phosphorylated and cystaminic hyaluronans the procedure reported by Cowman and Matsuoka was used. It consists in determining the specific viscosity to obtain, first the intrinsic viscosity and then the molecular weight (Kuo, 2006). To check the method consistency, the same procedure was performed on native hyaluronan whose molecular weight was known. A good accordance was found. In fact, its nominal MW was  $1.20 \times 10^6 \text{ D}$  and from the equation it resulted  $1.16 \times 10^6$  (i.e.: 1161116 D). MW of HAP was  $1.14 \times 10^6 \text{ D}$  (i.e.: 1138098 D) confirming that no significant polymer

degradation occurred during the phosphorylation procedure. Finally, MW of PAHAC was  $1.23 \times 10^6 \text{ D}$  (i.e.: 1229987 D). This small increase confirmed the hypothesis of the presence of a very low amount of intermolecular crosslinks as evidenced by the high fluidity index.

The rheological analysis pointed out that among the synthesised hyaluronan derivatives HAP was the only one still valuable as potential component of eye drops formulation. Furthermore, it showed increased rheological performance with respect native HA and commercial tears drops.

Consequently, further analysis in terms of thermogravimetric analysis, cytotoxicity and enzymatic degradation rate were performed on HAP only.

### 3.5. Thermogravimetric analysis

Thermographs of native and phosphorylated hyaluronan together with that of  $\text{NaH}_2\text{PO}_4$  are showed in Fig. 4. The derivative of the weight was plotted versus temperature to enhance

**Table 2**

Fluidity index and apparent viscosity of native and derivatised HA compared with a HA based commercial tear drop formulation.

Sample	N	$\eta_A$ (mPa s)		
		$D = 1 \text{ s}^{-1}$	$D = 100 \text{ s}^{-1}$	$D = 10,000 \text{ s}^{-1}$
HA	$0.7203 \pm 0.0005$	$105.4 \pm 0.5$	$20.3 \pm 0.2$	$8 \pm 1$
Commercial tears	$0.9686 \pm 0.0008$	$24.4 \pm 0.4$	$13.9 \pm 0.6$	$18.3 \pm 0.5$
HAP	$0.9924 \pm 0.0003$	$20.5 \pm 0.1$	$6.9\text{E-}3 \pm 0.4\text{E-}3$	$19.2 \pm 0.1$
PAHAC	$1.4031 \pm 0.0005$	$20.4 \pm 0.2$	$3.9\text{E-}4 \pm 0.1\text{E-}4$	$834.2 \pm 0.3$

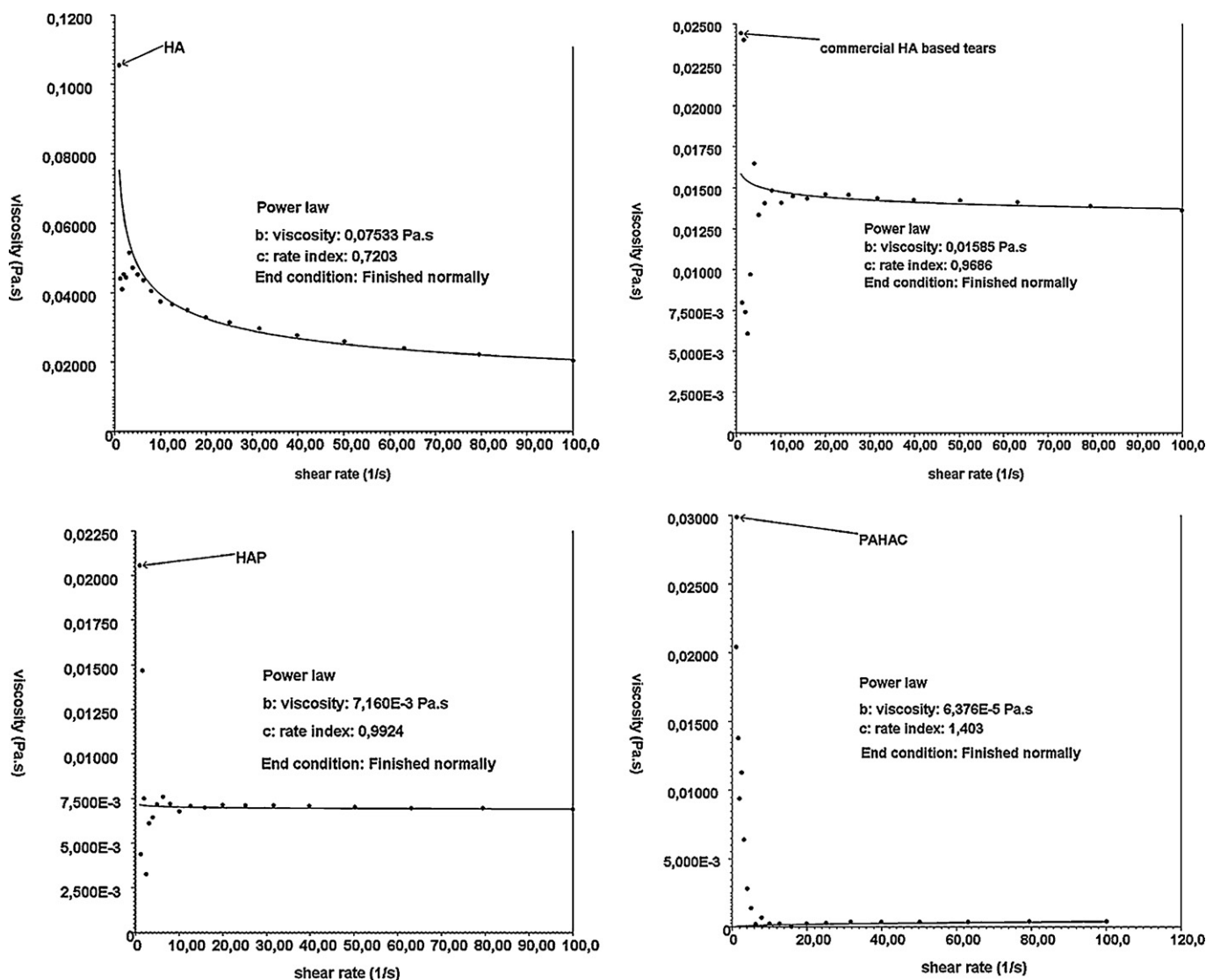


Fig. 3. Viscosity curve of 0.1% aqueous solution of: HA (A); commercial HA based tear drops (B); HAP (C) and PAHAC (D).

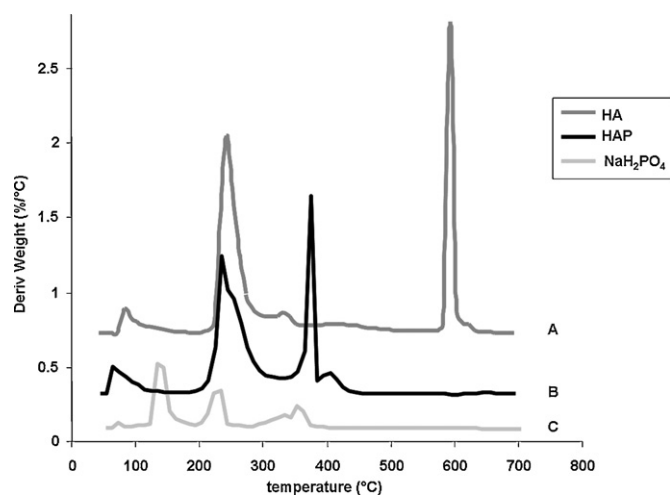
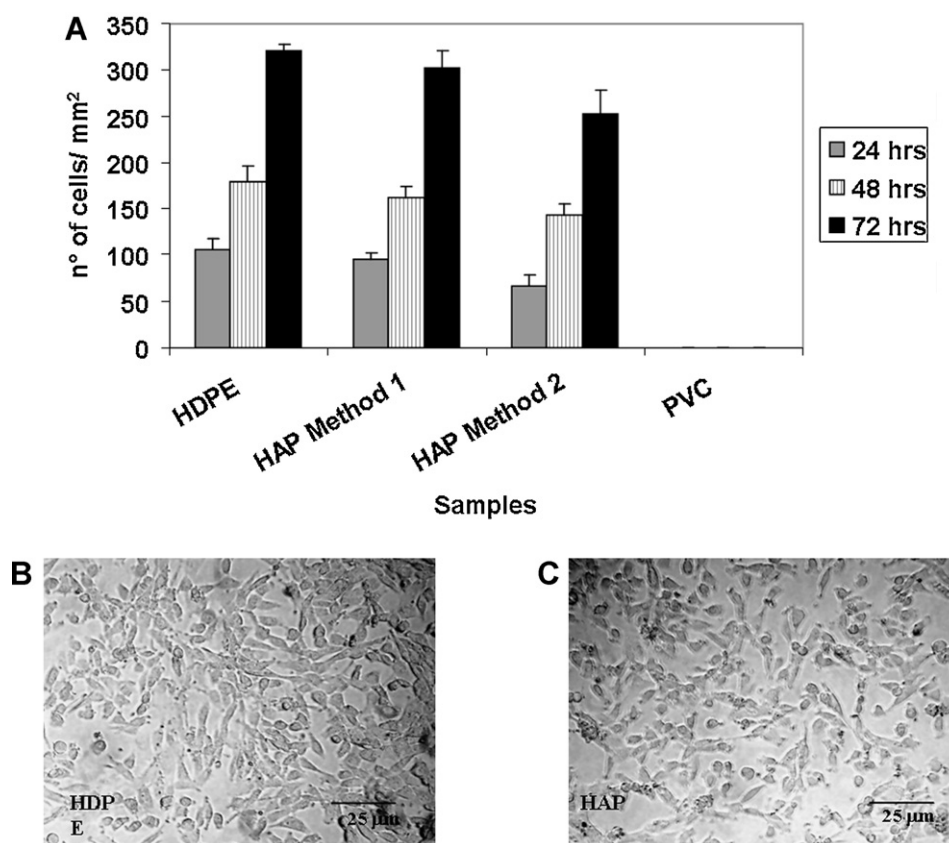


Fig. 4. Thermographs obtained plotting the derivative of weight versus temperature of HA (A); HAP (B) and  $\text{NaH}_2\text{PO}_4$  (C).

the weight changes. We analysed the thermal decomposition of  $\text{NaH}_2\text{PO}_4$  instead of that of STMP due to the greater similarity of the former to the polysaccharide chain phosphate groups.

The total weight loss of the two polymers, registered in the 40–700 °C range, is similar being  $76.5 \pm 0.4\%$  for HA and  $79.3 \pm 0.4\%$  for HAP. For both HA and HAP weight loss takes place in three stages. The first one, ranging from 40 to 120 °C, is assigned to the loss of free water and water linked through hydrogen bonds and depending on the humidity state of the sample. HA showed a weight loss of  $4.9 \pm 0.2\%$  whereas HAP showed a weight loss of  $9.2 \pm 0.5\%$ . The presence of phosphate groups along the chain provokes an increase of the polysaccharide hydrophilicity. Moreover, being the polymer negatively charged, the chain repulsion and stretching are also increased, thus permitting an increase of chains hydration. Furthermore, in this range of temperature a partial decomposition of phosphate is observed (Fig. 4C), thus increasing the overall weight loss observed in HAP in 40–120 °C range.

The second stage, ranging from 200 to 400 °C, corresponds to the thermal and oxidative decomposition of hyaluronan and vaporisation and elimination of volatile products. The relative weight loss for HA and HAP were  $46.4 \pm 0.4\%$  and  $67.1 \pm 0.3\%$ , respectively. Comparing the two thermographs reported in Fig. 4A and B with that reported in Fig. 4C we can see that the weight loss in HAP,



**Fig. 5.** (A) Number of adhered NIH3T3 in contact with HAP as a function of incubation time evaluated by optical microscopy cell count. The experiment was performed by following method 1 and method 2. Data are means  $\pm$  SD of five counts for each sample tested in triplicate. No value was statistically different versus control (HDPE); (B) Optical microscopy image of NIH3T3 after 72 h of culture in contact with HDPE (magnification 20 $\times$ ); (C) Optical microscopy image of NIH3T3 after 72 h of culture in contact with HAP (magnification 20 $\times$ ).

also in this temperature range, is due to both polysaccharidic and phosphate component. The third weight change occurring between 400 °C and 700 °C is related to the pyrolysis of the residual carbon and the elimination of water in crystal structure of the residue. It is known that pyrolysis of polysaccharides starts by a random split of the glycosidic bonds, followed by further decomposition forming acetic and butyric acids and a series of lower fatty acids, where C2, C3, and C6 predominate (Nieto, Peniche-Covas, & Padroin, 1991). The relative weight loss for HA and HAP were  $27.8 \pm 1.4\%$  and  $2.2 \pm 0.1\%$ , respectively.

This results agreed with the observation that HA decomposition residue was mainly sodium carbonate, whereas the presence of phosphate groups along the chains drastically affect the residue and decomposition fragments composition.

Finally, the differences in peak position, indicated that HAP differs in its holding capacity and in the strength of water–polymer interaction with respect to HA. In particular, the second stage of degradation shows peaks with maxima at 236 °C and at 230 °C for HA and HAP, respectively, indicating a thermal stability decrease of phosphorylated derivative in comparison with pure HA. Furthermore, the pyrolysis of HAP started at 320 °C and the weight became constant at 400 °C, while the HA shows the decomposition in the 570–630 °C range. The peak positions are expected to reflect physical and molecular changes caused by the modification of the polysaccharides (Neto et al., 2005). Consequently, this difference can be attributed mainly to the difference in chemical composition of the residue, even if a contribution may be also assigned to the hydrogen bond network destabilised by the introduction of phosphate groups as evidenced also by infrared analysis.

### 3.6. *In vitro* cytotoxicity, cell proliferation and viability

The evaluation of the *in vitro* acute toxicity does not depend on the final use for which the material is intended, and the document ISO 10993-5 recommends many cell lines from American Type Culture Collection (International Standard ISO 10993-5). HAP was tested for its potential cytotoxic effect and influence towards cell adhesion and growth on tumoral mouse fibroblasts (NIH3T3). HAP was found to be not cytotoxic for mouse fibroblast 3T3 and did not interfere with cell growth when added to both adherent (method 2) and not adherent (method 1) cells. In fact, the number of adhered cells/mm<sup>2</sup> in contact with the polymer was not statistically different in comparison with the negative control (HDPE) and it increased by increasing the incubation time (Fig. 5A).

The cell density trend was also confirmed by optical microscopy images. In fact, no significant difference of cell density on HDPE (Fig. 5B) and HAP (Fig. 5C) was found after 72 h of incubation. Images related only to method 1 have been reported since no difference was observed between method 1 and method 2. Furthermore, NIH3T3 showed an excellent spreading and their density increased with increasing the incubation time in both the samples. Finally, no signs of cytotoxicity, such as cell lysis were found.

### 3.7. Enzymatic degradation

The hyaluronidases are a group of enzymes distributed throughout the animal kingdom. Karl Meyer introduced the term “hyaluronidase” to denote the enzymes that degrade HA, and classified them into three different groups based on biochemical analysis and generated end products (Meyer, 1971). In this study we utilised



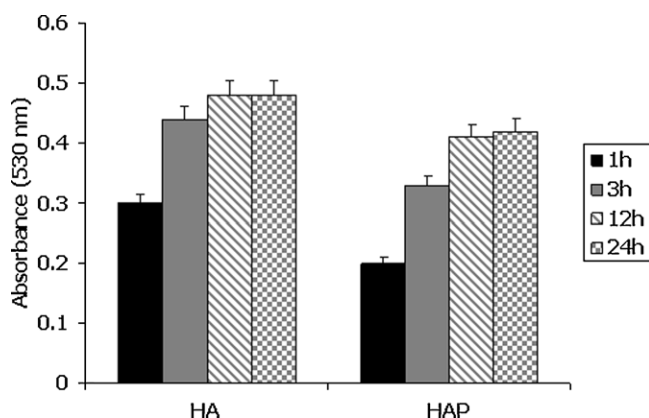


**Fig. 6.** Measured absorbance values ( $\lambda = 530$  nm) of the uronic residues produced during HA hydrolysis by hyaluronidase for the different digestion time (from 1 to 24 h).

enzymes from *Streptomyces hyalurolyticus* (Ohya & Kaneko, 1970; Shimada & Matsumura, 1980). This enzyme is entirely different from other bacterial hyaluronidases because of its absolute specificity for HA. Furthermore, these  $\beta$ - endoglycosidases, that specifically cleave the  $\beta$ -(1 $\rightarrow$ 4) linkage in HA, act with a mechanism of action entirely different from that of the eukaryotic glycoside hydrolases. These enzymes act by  $\beta$ - elimination with introduction of an unsaturated bond (EC 4.2.99.1) (Jedrzejewski, 2004; Stern & Jedrzejewski, 2006). The generation of the double bond enables to perform a spectrophotometric assay, which is not available for the eukaryotic enzymes, which act hydrolytically.

In Fig. 6 the measured absorbance values are reported at different digestion times (from 1 to 24 h). The graph pointed out that HAP showed an increased resistance to degradation, in terms of production of uronic acid, as induced by hyaluronidase. In fact, native hyaluronan, (HA) was significantly degraded after only 3 h by hyaluronidase and subsequent digestion up to 24 h did not produce any other significant amount of uronic acid. This behaviour suggested that the digestion of hyaluronan by hyaluronidase is almost complete in the very first 2–3 h of contact, according to the literature (He, Zhou, Wei, Nie, & Yao, 2001). On the contrary, the phosphate derivative never reached the degradation level of the control within the first 24 h of contact with hyaluronidase.

The effect of phosphate groups along the hyaluronan chains confirmed the effect of negatively charged groups. Sulphated hyaluronan showed a similar behaviour (Abatangelo, Barbucci, Brun, & Lamponi, 1997). It is well known that hyaluronidases attack the hyaluronan chain degrading the glycosidic bonds. The presence of negatively charged groups seems to hinder the site attack.

#### 4. Conclusion

We synthesised two hyaluronan derivatives containing cystaminic or phosphate groups along the chains. This study has revealed that only phosphorylated hyaluronan shows rheological properties adequate to the application as eye drops. In fact, its apparent viscosity at a shear rate of  $10,000\text{ s}^{-1}$  is higher than the threshold value of 10 mPa s, but lower than the value which induces a sticky sensation and irritation (i.e. 30 mPa s). Thermo-gravimetric analysis has pointed out a drastic decrease in the hydrogen bond network by introducing phosphate groups, thus permitting a higher mobility and hydration of polysaccharide chains. The phosphorylated derivative is not cytotoxic and it is able to drastically reduce hyaluronidase attack towards hyaluronan chain. All these properties make HAP derivative as a potential adjuvant for tear drops formulations or as a vehicle for ophthalmic

drugs since phosphorylation involves hydroxyl groups leaving the carboxylic groups free to be further modified. The phosphorylated polymer could be crosslinked, thus creating a vehicle for specific biomolecules whose release could be controlled due to the slower degradation of polysaccharidic chains by hyaluronidases.

#### Acknowledgment

The Italian Interuniversity Consortium CSGI supported the research.

#### Appendix A. Supplementary data

Supplementary data associated with this article can be found, in the online version, at doi:10.1016/j.carbpol.2011.12.047.

#### References

- Abatangelo, G., Barbucci, R., Brun, P., & Lamponi, S. (1997). Biocompatibility and enzymatic degradation studies on sulphated hyaluronic acid derivatives. *Biomaterials*, 18, 1411–1415.
- Barbucci, R., Consumi, M., & Magnani, A. (2002). Dependence of water uptake and morphology of hyaluronan- and alginate-based hydrogels on pH and degree of crosslinking. *Macromolecular Chemistry and Physics*, 203, 1292–1300.
- Barbucci, R., Leone, G., Monici, M., Pantalone, D., Fini, M., & Giardino, R. (2005). The effect of amidic moieties on polysaccharides: evaluation of the physicochemical and biological property of amidic carboxymethylcellulose (CMCA) in the form of linear polymer and hydrogel. *Journal of Material Chemistry*, 15, 2234–2241.
- Bellamy, L. J. (1980). *The infrared spectra of complex molecules* (2nd ed.). London: Chapman and Hall Ltd.
- Bitter, T., & Muir, H. M. (1962). A modified uronic acid carbazole reaction. *Analytical Biochemistry*, 4, 330–334.
- Chrai, S. S., & Robinson, J. R. (1974). Ocular evaluation of methylcellulose vehicle in albino rabbits. *Journal Pharmaceutical Science*, 63, 1218–1223.
- Cowman, M. K., & Matsuoka, S. (2005). Experimental approaches to hyaluronan structure. *Carbohydrate Research*, 340, 791–809.
- DeNoyer, L. K., & Dodd, J. G. (2002). Smoothing and derivatives in spectroscopy. In J. M. Chalmers, & P. R. Griffiths (Eds.), *Handbook of vibrational spectroscopy: sample characterization and spectral data processing* (pp. 2173–2184). New York: John Wiley and Sons, Ltd.
- Dulong, V., Lack, S., Le Cerf, D., Picton, L., Vannier, J. P., & Muller, G. (2004). Hyaluronan-based hydrogels particles prepared by crosslinking with trisodium trimetaphosphate. Synthesis and characterisation. *Carbohydrate Polymer*, 57, 1–6.
- Durrani, A. M., Farr, S. J., & Kellaway, I. W. (1995). Influence of molecular weight and formulation pH on the precorneal clearance rate of hyaluronic acid in the rabbit eye. *International Journal of Pharmaceutical*, 118, 243–250.
- Frey, B. L., Hanken, D. G., & Corn, R. M. (1993). Vibrational spectroscopic studies of the attachment chemistry for zirconium phosphonate multilayers at gold and germanium surfaces. *Langmuir*, 9, 1815–1820.
- Griffiths, P. R., & De Haseth, J. A. (2007). *Fourier transform infrared spectrometry* (2nd ed.). New Jersey: Wiley-Interscience.
- Haxaire, K., Marechal, Y., Milas, M., & Rinaudo, M. (2003). Hydration of polysaccharide hyaluronan observed by IR spectrometry preliminary experiments and band assignment. *Biopolymer Biospectroscopy*, 72, 10–20.
- He, D., Zhou, A., Wei, W., Nie, L., & Yao, S. (2001). A new study of the degradation of hyaluronic acid by hyaluronidase using quartz crystal impedance technique. *Talanta*, 53, 1021–1029.
- Hedberg, E. L., Shih, C. K., Solchaga, L. A., Caplan, A. I., & Mikos, A. G. (2004). Controlled release of hyaluronan oligomers from biodegradable polymeric microparticle carriers. *Journal of Controlled Release*, 100, 257–266.
- International Standard ISO 10993-5, 1st ed. ISO, Geneva (1992).
- Jedrzejewski, M. J. (2004). Extracellular virulence factors of *Streptococcus pneumoniae*. *Frontiers in Bioscience*, 9, 891–914.
- Jia, X., Burdick, J. A., Kobler, J., Clifton, R. J., Rosowski, J. J., Zeitels, S. M., & Langer, R. (2004). Synthesis and characterization of in situ cross-linkable hyaluronic acid-based hydrogels with potential application for vocal fold regeneration. *Macromolecules*, 37, 3239–3248.
- Kragten, E. A., Leeflang, B. R., Kamerling, J. P., & Vliegthart, J. F. G. (1992).  $^1\text{H}$  NMR spectroscopy of O-carboxymethyl derivatives of D-glucose. *Carbohydrate Research*, 228, 433–437.
- Kristiansen, K. A., Potthast, A., & Christensen, B. E. (2010). Periodate oxidation of polysaccharides for modification of chemical and physical properties. *Carbohydrate Research*, 345, 1264–1271.
- Kuo, J. W. (2006). *Practical aspects of hyaluronan based medical products*. Boca Raton, FL, USA: CRC Press. (pp. 9–10)
- Leone, G., Consumi, M., Aggravi, M., Donati, A., Lamponi, S., & Magnani, A. (2010). PVA/STMP based hydrogels as potential substitutes of human vitreous. *Journal of Materials Science: Materials in Medicine*, 21, 2491–2500.

- Leone, G., Torricelli, P., Giardino, R., & Barbucci, R. (2008). New phosphorylated derivatives of carboxymethylcellulose with osteogenic activity. *Polymer Advanced Technology*, 19, 824–830.
- Ludwig, A. (2005). The use of mucoadhesive polymers in ocular drug delivery. *Advanced Drug Delivery Review*, 57, 1595–1639.
- Ludwig, A., & Van Ooteghem, M. (1989). Evaluation of sodium hyaluronate as viscous vehicle for eye drops. *Journal of Pharmacie de Belgique*, 44, 391–397.
- Magnani, A.; Rossi, C.; Consumi, M.; Greco, G. 2010. Derivati fosfatati di polisaccaridi e usi di essi. Italian Patent N.0001378966.(30.08.2010).
- Maurice, D. M. (1973). The dynamics and drainage of tears. *International Ophthalmology Clinics*, 13, 103–116.
- Meyer, K. (1971). Hyaluronidases. In P.D. Boyer (Ed.), *The enzymes* (3rd ed., Vol. v, pp. 307–320). New York: Academic Press.
- Neto, C. G. T., Giacometti, J. A., Job, A. E., Ferreira, F. C., Fonseca, J. L. C., & Pereira, M. R. (2005). Thermal analysis of chitosan based networks. *Carbohydrate Polymers*, 62, 97–103.
- Nieto, J. M., Peniche-Covas, C., & Padroin, G. (1991). Characterization of chitosan by pyrolysis-mass spectrometry, thermal analysis and differential scanning calorimetry. *Thermochimica Acta*, 176, 63–68.
- Oechsner, M., & Keipert, S. (1999). Polyacrylic/polyvinylpyrrolidone bipolymeric systems I rheological and mucoadhesive properties of formulations potentially useful for the treatment of dry-eye-syndrome. *European Journal of Pharmaceutics and Biopharmaceutics*, 47, 113–118.
- Ohya, T., & Kaneko, Y. (1970). Novel hyaluronidase from streptomyces. *Biochimica et Biophysica Acta*, 198, 607–609.
- Ravanelle, F., Marchessault, R. H., Legare, A., & Buschmann, M. D. (2002). Mechanical properties and structure of swollen crosslinked high amylose starch tablets. *Carbohydrate Polymers*, 47, 259–266.
- Saad, O. M., Myers, R. A., Castleton, D. L., & Leary, J. A. (2005). Analysis of hyaluronan content in chondroitin sulfate preparations by using selective enzymatic digestion and electrospray ionization mass spectrometry. *Analytical Biochemistry*, 344, 232–239.
- Shimada, E., & Matsumura, G. (1980). Degradation process of hyaluronic acid by Streptomyces hyaluronidase. *Journal of Biochemistry*, 88, 1015–1023.
- Smith, B. C. (1996). *Fundamentals of Fourier-transform infrared spectroscopy*. Boca Raton, FL, USA: CRC, Press.
- Snibson, G. R., Greaves, J. L., Soper, N. D., Prydal, J. I., Wilson, C. G., & Bron, A. J. (1990). Precorneal residence times of sodium hyaluronate solutions studied by quantitative gamma scintigraphy. *Eye*, 4, 594–602.
- Stern, R., & Jedrzejewski, M. J. (2006). Hyaluronidases: their genomics, structures, and mechanisms of action. *Chemical Reviews*, 106, 818–839.
- Thomas, L. C., & Chittenden, R. A. (1964). Characteristic infrared absorption frequencies of organophosphorus compounds—II P...O... (X) bonds. *Spectrochimica Acta*, 20, 489–502.
- Virender, K. S., Kent, S. B. H., Tam, J. P., & Merrifield, R. B. (1981). Quantitative monitoring of solid-phase peptide synthesis by the ninhydrin reaction. *Analytical Biochemistry*, 117, 147–157.
- Yokoi, N., & Komuro, A. (2004). Non-invasive methods of assessing the tear film. *Experimental Eye Research*, 78, 399–407.
- Zaki, I., Fitzgerald, P., Hardy, J. G., & Wilson, C. G. (1986). A comparison of the effect of viscosity on the precorneal residence of solutions in rabbit and man. *Journal of Pharmacy Pharmacology*, 38, 463–466.
- Zhu, H., & Chauhan, A. (2008). Effect of viscosity on tear drainage and ocular residence time. *Optometry and Vision Science*, 85, E715–E725.